

# Proline hydroxylation and C-terminal amidation in $\mu$ -conotoxins increase structural stability and potency at sodium channels

Victoria A. Adegoke<sup>A</sup>, Yashad Dongol<sup>B</sup>, Tye Gonzalez<sup>A</sup>, Angela Song<sup>A</sup>, Richard J. Clark<sup>A</sup>, Richard J. Lewis<sup>B</sup> , Anne C. Conibear<sup>A,C,\*</sup>  and K. Johan Rosengren<sup>A,\*</sup>

For full list of author affiliations and declarations see end of paper

**\*Correspondence to:**

Anne C. Conibear  
 Institute of Applied Synthetic Chemistry,  
 Faculty of Technical Chemistry, TU Wien,  
 Getreidemarkt 9, A-1060 Vienna, Austria  
 Email: [anne.conibear@tuwien.ac.at](mailto:anne.conibear@tuwien.ac.at)

K. Johan Rosengren  
 School of Biomedical Sciences, Faculty of  
 Medicine, The University of Queensland,  
 Saint Lucia, Qld 4072, Australia  
 Email: [j.rosengren@uq.edu.au](mailto:j.rosengren@uq.edu.au)

**Handling Editor:**

Mibel Aguilar

**Received:** 30 April 2025

**Accepted:** 22 July 2025

**Published:** 2 September 2025

**Cite this:** Adegoke VA *et al.* (2025) Proline hydroxylation and C-terminal amidation in  $\mu$ -conotoxins increase structural stability and potency at sodium channels. *Australian Journal of Chemistry* **78**, CH25071. doi:10.1071/CH25071

© 2025 The Author(s) (or their employer(s)).  
 Published by CSIRO Publishing.  
 This is an open access article distributed  
 under the Creative Commons Attribution-  
 NonCommercial 4.0 International License  
 (CC BY-NC)

OPEN ACCESS

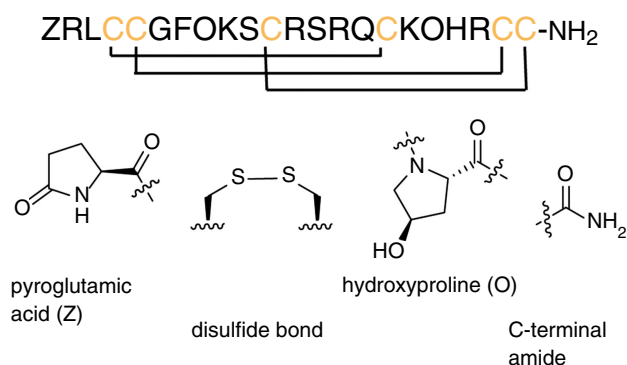
## ABSTRACT

Conotoxins are disulfide-rich peptides isolated from the venoms of marine cone snails. These natural products have inspired the development of several drug candidates and novel therapeutic leads. In addition to disulfide bonds, many conotoxins are highly modified with posttranslational modifications (PTMs) such as proline hydroxylation, C-terminal amidation and glycosylation, among others. These modifications can alter the charge, size and hydrophobicity of the conotoxin, influencing its interaction with target receptors and modulating its potency and selectivity. PTMs can also affect the folding kinetics and conformational stability of the peptide, which further affects its biological activity. Although conotoxins undergo a variety of PTMs, the functions of many of these modifications remain unclear. Here, we explored the structural and functional implications of PTMs in two representative conotoxins, PIIIA and TIIIA of the  $\mu$ -pharmacological family. We synthesised a series of PIIIA and TIIIA peptides bearing native hydroxyproline and C-terminal amidation PTMs, along with their unmodified counterparts. Solid phase peptide synthesis and non-selective disulfide bond formation provided access to pure forms of the eight possible variants for *in vitro* comparison of their oxidative folding. Structural studies using nuclear magnetic resonance (NMR) spectroscopy, alongside electrophysiological and serum stability assays, were conducted to characterise the functional roles of the PTMs in these conotoxins. Our results suggest that, whereas C-terminal amidation has a crucial role in folding and structural integrity, proline hydroxylation significantly influences the *in vitro* oxidative folding, stability and biological activity of these conotoxin peptides.

**Keywords:** C-terminal amidation,  $\mu$ -conotoxins, nuclear magnetic resonance spectroscopy, oxidative folding, posttranslational modification, proline hydroxylation, sodium channels, solid phase peptide synthesis, structure–function relationship.

## Introduction

Conotoxins are peptides derived from the venom of marine cone snails (*genus Conus*) and represent a rich and diverse source of bioactive compounds. These venoms are used by the cone snails to defend themselves, deter competitors and capture their prey. A single injection of venom often contains over 1000 bioactive peptides.<sup>1–3</sup> Owing to their remarkable specificity and potency in modulating ion channels, receptors and other extracellular targets, these peptides have garnered significant interest as valuable tools for pharmacological research and as potential therapeutic agents. Conotoxins can be categorised in three ways: classification according to their gene superfamily, pharmacological families or cysteine framework.<sup>4–6</sup> Within the diverse pharmacological families of conotoxins,  $\mu$ -conotoxins stand out for their remarkable ability to selectively inhibit voltage-gated sodium channels (Nav). Typically comprising 12–24 amino acid residues, the  $\mu$ -conotoxins are among the most prevalent and well-characterised conotoxins.<sup>7</sup> Their disulfide-rich



**Fig. 1.** Conotoxin PIIIA is a component of the venom of marine cone snails. The amino acid sequence of PIIIA is presented (pyroglutamic acid = Z, hydroxyproline = O), with cysteine residues in yellow and disulfide connectivities shown as lines. The lower panel shows the chemical structures of posttranslational modifications (PTMs) in PIIIA and many other members of the  $\mu$ -conotoxin family.

structures feature a conserved six-cysteine framework (CC-C-C-CC) with a native connectivity pattern of C1-C4, C2-C5 and C3-C6 (Fig. 1).<sup>8</sup> The cysteine framework significantly enhances their structural stability, making them valuable tools for pharmacological research and for potential therapeutic applications.<sup>9-11</sup> The specificity in targeting Nav channel subtypes, such as Nav1.7, which is closely linked to pain pathways, underscores their potential in the development of analgesics.<sup>12</sup> Studies have also demonstrated that  $\mu$ -conotoxins can effectively block the pore of Nav channels from the extracellular side, thereby inhibiting sodium ion flow and altering neuronal excitability.<sup>13</sup> This mechanism positions  $\mu$ -conotoxins as promising candidates for treating conditions such as epilepsy and chronic pain, where selective sodium channel modulation is critical.<sup>11,14</sup>

The functional diversities and potencies of  $\mu$ -conotoxins are not solely attributed to their primary sequences but are significantly influenced by posttranslational modifications (PTMs). PTMs are modifications to amino acids that are not explicitly encoded in the gene associated with a peptide.<sup>15,16</sup> Such modifications, in addition to the formation of disulfide bonds, are abundant and diverse in conotoxins and can be crucial for regulating their structures, stabilities and pharmacological properties. These PTMs include glycosylation, hydroxylation, oxidation, cysteine modifications and  $\gamma$ -carboxylation, among others (Fig. 1).<sup>4,17</sup> The specific PTMs that conotoxins undergo vary depending on their target ion channels or receptors. For instance, most  $\mu$ -conotoxins, which target Nav channels, undergo C-terminal amidation, whereas proline hydroxylation in  $\mu$ -conotoxins is less prevalent. Both PTMs have been found to have crucial roles in the stabilities and potencies of these conotoxins at sodium channels.<sup>18,19</sup>

Proline hydroxylation is a PTM that involves the enzymic addition of a hydroxyl group to the beta or gamma carbon of a

proline residue, converting it into hydroxyproline (one-letter code 'O').<sup>15,20</sup> In mammalian systems, prolyl 4-hydroxylase (PH4) catalyses this modification; however, the enzyme responsible for proline hydroxylation in cone snails remains uncharacterised. Hydroxyproline residues and their stereochemistry have a crucial role in conotoxins by influencing peptide conformation, stability and oxidative folding, which are essential for their biological activity and target interactions.<sup>21,22</sup> For instance, the incorporation of hydroxyproline into  $\alpha$ -conotoxins has been associated with enhanced binding affinity and specificity for receptors involved in neuromuscular signaling,<sup>23</sup> as well as improved *in vitro* oxidative folding and stability of certain conotoxins.<sup>18</sup>

C-terminal amidation, another important PTM in conotoxins, is primarily catalysed by the enzyme peptidylglycine  $\alpha$ -amidating monooxygenase (PAM), also known as peptidylglycine hydroxylase (PHM), which plays a vital role in the biosynthesis and activity of many bioactive peptides. Additionally, it prevents degradation by exopeptidases and increases the activity of conotoxins at their target receptors, influencing their interactions with binding partners.<sup>24,25</sup> This modification has been shown to affect the analgesic properties of certain conotoxins, highlighting its significance in modulating their biological effects and to cause slight conformational changes at the C-terminus of  $\alpha$ -conotoxins.<sup>26,27</sup> To our knowledge, no  $\mu$ -conotoxin lacking the C-terminal amide has been structurally or functionally characterised in the literature.

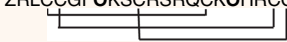

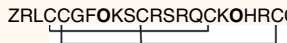
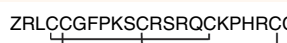
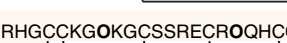
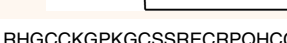
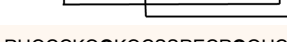
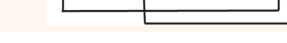
In this work, we investigated the role of proline hydroxylation and C-terminal amidation in the folding, structure, stability and activities of two  $\mu$ -conotoxins, PIIIA and TIIIA, belonging to the M gene superfamily and the  $\mu$ -pharmacological family. Both  $\mu$ -conotoxins are known for their ability to selectively target and inhibit Nav channels. PIIIA additionally has an N-terminal pyroglutamic acid modification (one-letter code 'Z'), which was included, but not explicitly investigated in this study. Variants of the  $\mu$ -conotoxins with and without native hydroxyproline and C-terminal amidation PTMs were synthesised and their *in vitro* oxidative folding and disulfide bond formation were compared. The role of the PTMs in their structures was investigated using NMR spectroscopy, and serum stability assays were conducted to determine the functional role of these PTMs in the conotoxins. Additionally, activities of the PIIIA and TIIIA variants were measured on three human voltage-gated sodium channel subtypes, Nav1.2, Nav1.4 and Nav1.7 human sodium channels (hNav) using electrophysiology. These studies showed that C-terminal amidation and proline hydroxylation influence the *in vitro* oxidative folding, overall structure, stability and bioactivity of the  $\mu$ -conotoxins PIIIA and TIIIA. In addition to extending our understanding of the intrinsic structures and activities of these  $\mu$ -conotoxins, this study underscores the significance of conotoxins as valuable model peptides for elucidating the individual and combined effects of PTMs.

## Results

### Peptide synthesis, purification and oxidative folding

Using solid phase peptide synthesis, we synthesised four variants each of the PIIIA and TIIIA peptides with and without the two native hydroxyproline PTMs and C-terminal amidation (Table 1) and purified the respective reduced forms. The peptides were then subjected to undirected oxidative folding, a method previously shown to be effective for the formation of three disulfide bonds in native PIIIA and TIIIA peptides.<sup>28,29</sup> Oxidation of the native PIIIA and TIIIA variants bearing hydroxyproline PTMs and C-terminal amidation, and their proline counterparts (Pro8,18)PIIIA and (Pro8,18)TIIIA, resulted in the formation of multiple disulfide isomers; however, these could be separated by RP-HPLC and analysed by NMR spectroscopy to confirm folding. Oxidation of the acid variants (lacking C-terminal amidation) of the PIIIA and TIIIA peptides with and without hydroxyproline PTMs (PIIIA-OH, (Pro8,18)PIIIA-OH, TIIIA-OH and (Pro8,18)TIIIA-OH) was attempted using similar conditions. Although several products were isolated by RP-HPLC, the NMR data of all isomers suggested misfolded peptides. Consequently, a range of oxidising conditions were explored<sup>29–35</sup> but the NMR data of all purified isomers indicated misfolded peptides, as evidenced by poor dispersion of amide signals, multiple conformations and non-native disulfide connectivities, despite the mass spectra confirming the formation of three disulfide bonds. We therefore proceeded to compare the hydroxyproline- and proline-containing variants of each of the conotoxins PIIIA and TIIIA bearing the C-terminal amidation.

**Table 1.** Sequences and nomenclature of the  $\mu$ -conotoxin peptide variants synthesised in this study.

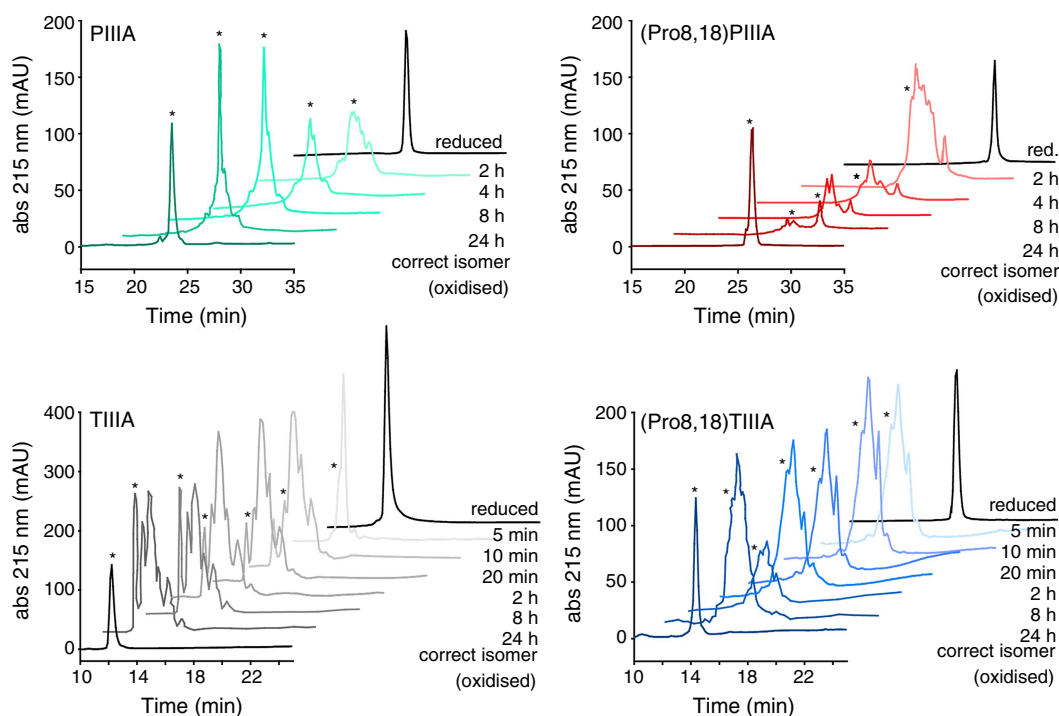
Peptide	Sequence
PIIIA (native)	ZRLCCG <b>F</b> OKSCRSRQCKOHRCC-NH <sub>2</sub> 
(Pro8,18)PIIIA	ZRLCCG <b>F</b> PKSCRSRQCKPHRCC-NH <sub>2</sub> 
PIIIA-OH	ZRLCCG <b>F</b> OKSCRSRQCKOHRCC-OH 
(Pro8,18)PIIIA-OH	ZRLCCG <b>F</b> PKSCRSRQCKPHRCC-OH 
TIIIA (native)	RHG <b>C</b> CKGOKGCSSRECRQHC-NH <sub>2</sub> 
(Pro8,18)TIIIA	RHG <b>C</b> CKGPKGCSSRECRPQHCC-NH <sub>2</sub> 
TIIIA-OH	RHG <b>C</b> CKGOKGCSSRECRQHC-OH 
(Pro8,18)TIIIA-OH	RHG <b>C</b> CKGPKGCSSRECRPQHCC-OH 

Z, Pyroglutamic acid; **O**, Hydroxyproline.

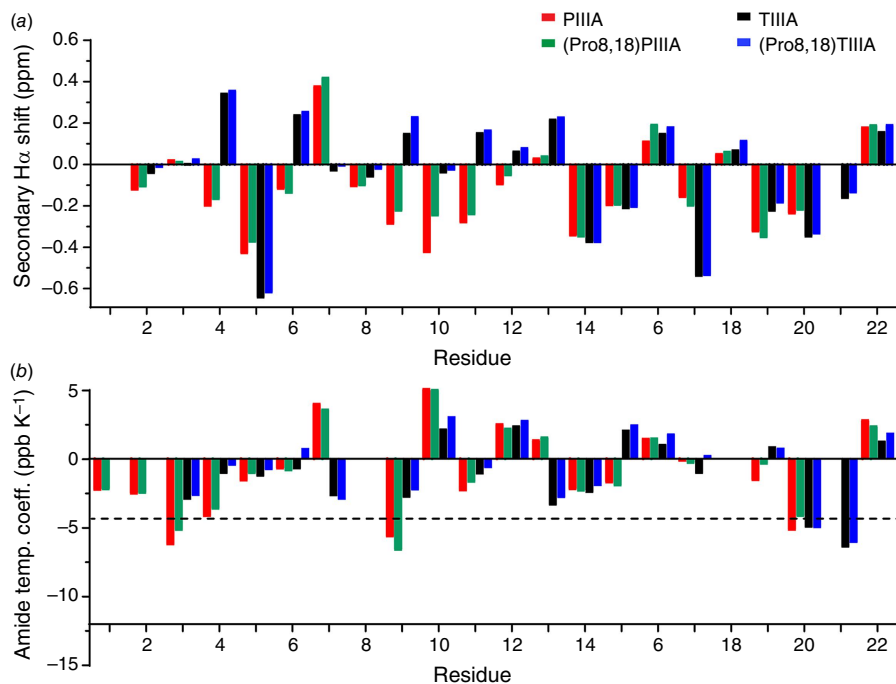
To compare the oxidation kinetics of the C-terminal amidated PIIIA and TIIIA  $\mu$ -conotoxin variants with and without hydroxyproline PTMs, the oxidative folding reaction mixture was sampled at selected timepoints over 24 h, followed by quenching with 4% TFA in water. The RP-HPLC traces were recorded and compared to those of the corresponding pure reduced form and the oxidised form with the desired native disulfide connectivity as identified by NMR spectroscopy (Fig. 2 and Supplementary Fig. S1). The PIIIA and (Pro8,18)PIIIA peptides showed similar folding rates and both produced several disulfide isomers of the fully oxidised products, as confirmed by mass spectrometry. However, as confirmed by NMR spectroscopy, the native PIIIA peptide yielded a higher proportion of the correctly folded isomer (C1–C4, C2–C5 and C3–C6) compared to the unmodified (Pro8,18)PIIIA, which showed more isomers with non-native disulfide connectivities. The oxidative folding of the TIIIA hydroxyproline and proline variants occurred much faster than that of the PIIIA counterparts. Interestingly, we observed that the isomer with the native disulfide connectivity in the hydroxyproline-containing TIIIA takes longer to appear than for the (Pro8,18)TIIIA variant; however, the hydroxyproline-containing TIIIA peptide had better separation of the isomers, making it easier to isolate the correctly folded isomer. Taken together, these results suggest that proline hydroxylation as a PTM facilitates the *in vitro* oxidative folding and correct disulfide pairing of both the PIIIA and TIIIA  $\mu$ -conotoxins.

### NMR spectroscopy of the $\mu$ -conotoxin variants

The three-dimensional structures of  $\mu$ -conotoxins PIIIA and TIIIA have been previously elucidated using solution NMR spectroscopy.<sup>28,36</sup> To further investigate their structural characteristics, we analysed the amidated variants of PIIIA and TIIIA with and without hydroxyproline PTMs using homo-nuclear and heteronuclear NMR spectroscopy. Notable differences in the <sup>1</sup>H spectra were observed between the hydroxyproline and proline variants, including variations in signal dispersion, line widths and signal-to-noise ratios. Resonances were assigned from <sup>1</sup>H–<sup>1</sup>H TOCSY<sup>37</sup> and <sup>1</sup>H–<sup>1</sup>H NOESY<sup>38,39</sup> NMR spectra, supported by <sup>1</sup>H–<sup>13</sup>C<sup>40</sup> and <sup>1</sup>H–<sup>15</sup>N HSQC<sup>41</sup> spectra (representative spectra are shown in Supplementary Fig. S2–S5), following the sequential assignment protocol,<sup>42</sup> and were largely unambiguous. The PIIIA variants exhibited multiple conformations, especially for (Pro8,18)PIIIA, which complicated assignment of the spectra. These conformational states were attributed to *cis*–*trans* isomerisation at Pro8/Hyp8, with the *trans* isomer being predominant (Supplementary Fig. S6). By contrast, the 2-D NMR spectra of hydroxyproline-containing TIIIA and its proline counterpart (Pro8,18)TIIIA had narrow, well-dispersed peaks and many NOE cross-peaks, suggesting a single, well-defined conformation in solution. Importantly, both Hyp8 and Hyp18 in TIIIA exhibited strong sequential H $\delta$ –H $\alpha_{i-1}$



**Fig. 2.** *In vitro* oxidative folding of  $\mu$ -conotoxin variants with and without native hydroxyproline PTMs. RP-HPLC traces depicting the time-course of oxidative folding are shown with a 2-min offset on the x-axis between the time points. The fully oxidised form with the desired disulfide connectivity is marked with an asterisk (\*). Full RP-HPLC traces are shown in Supplementary Fig. S1.



**Fig. 3.** Secondary  $H_{\alpha}$  and temperature coefficients of  $\mu$ -conotoxin variants. (a) Secondary  $H_{\alpha}$  chemical shifts of hydroxyproline-containing PIIIA and TIIIA with their proline counterparts (Pro8,18)PIIIA and (Pro8,18)TIIIA. Significant deviations from random coil shifts (absolute values  $>0.1$  ppm) indicate structural order. Negative  $H_{\alpha}$  secondary shifts correspond to  $\alpha$ -helical regions and positive shifts indicate  $\beta$ -sheet regions. (b) Amide proton temperature coefficients of PIIIA, TIIIA, (Pro8,18)PIIIA and (Pro8,18)TIIIA. Amide protons with temperature coefficients lower than  $-4.6$  ppb  $K^{-1}$  (dashed line) have an 85% likelihood of participating in hydrogen bonding as donors. Amide proton signals of residues 1 and 2 in TIIIA and (Pro8,18)TIIIA are not detected due to fast exchange. Residues 8 and 18 correspond to hydroxyproline and proline respectively.

NOEs, confirming that they adopt a *trans* conformation, with no indications of the *cis* conformation. Backbone chemical shift assignments for all four amidated variants are given in the Supplementary Tables S1 and S2.

Secondary  $H_{\alpha}$  chemical shifts were obtained by subtraction of the random coil chemical shift values from the measured chemical shifts to compare the variants and identify secondary structural elements.<sup>43,44</sup> As shown in Fig. 3a,

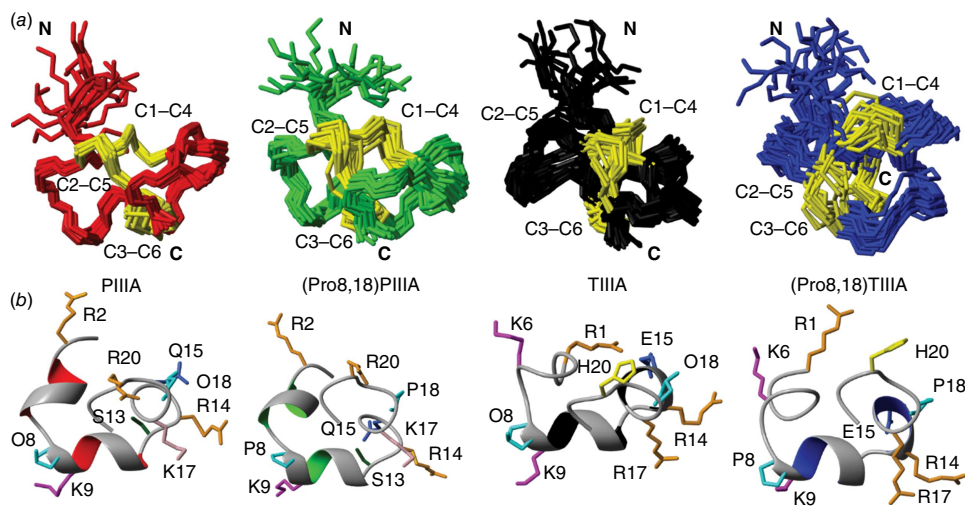
the series of negative  $H_{\alpha}$  shifts indicate short helices or turns and an overall lack of  $\beta$ -sheet content, consistent with the expected  $\mu$ -conotoxin structures. For the PIIIA and TIIIA hydroxyproline- and proline-containing variants, the backbone conformations are essentially the same, as shown by similar  $H_{\alpha}$  secondary shifts for the two variants. However, the hydroxyproline-containing PIIIA variant (red bars) has slightly more negative values than (Pro8,18)PIIIA (green bars) in the region 9–12, potentially indicating a more stabilised helical structure. Nevertheless, proline hydroxylation does not appear to significantly affect the overall secondary structure in either of the  $\mu$ -conotoxins.

Backbone amide hydrogen bond restraints were determined by calculating temperature coefficients.<sup>45</sup> The hydroxyproline-containing PIIIA and TIIIA variants exhibit almost identical temperature coefficients to their respective (Pro8,18)PIIIA and (Pro8,18)TIIIA counterparts (Fig. 3b), suggesting the same hydrogen bond network. This implies that proline hydroxylation has a limited or negligible role in altering the backbone hydrogen bond network of the PIIIA and TIIIA peptides. The hydroxyl group in hydroxyproline might nevertheless be involved in hydrogen bonding with other side chains, or with the solvent.

To investigate the structural characteristics of the PIIIA and TIIIA variants, three-dimensional structures were determined from the NMR data. Hydrogen bond restraints derived from temperature coefficients, inter-proton distance restraints obtained from NOESY cross-peak volumes, analysis of preliminary structures, and backbone and side chain dihedral angles defined by TALOS-N (see <https://spin.niddk.nih.gov/bax/software/TALOS-N/>) and DISH ('disulfide and dihedral prediction', see [https://github.com/davarm/DISH\\_prediction](https://github.com/davarm/DISH_prediction)) were all combined for the structure calculations.<sup>46</sup> Preliminary structure calculations were carried out using automated NOE assignment within CYANA (ver. 3.98.15, see <https://cyana.org/>) and the final structure calculation and water minimisation were carried out in CNS ('Crystallography and NMR System',

ver. 1.21, see <https://cns-online.org/v1.3/>).<sup>46</sup> To assess the accuracy of the structural geometry and atom packing, the structures were examined using MolProbity (ver. 4.5.2, see <http://molprobity.biochem.duke.edu/>).<sup>47</sup> The 20 top structures out of the final set of 50 were chosen based on their MolProbity scores, low energy and absence of substantial experimental violations. Detailed statistical data from the calculations are provided in Supplementary Tables S3 and S4. It should be noted that NMR structures were calculated based on samples at pH ~3.5, to maximise sensitivity in the amide region of the spectra, whereas stability and activity assays were conducted at physiological pH 7.4. As the structures are constrained by the three disulfide bonds, we do not expect any major structural difference between the two pH values.

In agreement with predictions based on the  $H_{\alpha}$  secondary shifts, all four  $\mu$ -conotoxin variants showed well-ordered central regions characterised by a series of turns, with less structured N-terminal tails, which were more disordered in the proline-containing variants (Fig. 4). The latter is reflected in the RMSD values upon superimposing residues 3–22 of each of the peptides: PIIIA (0.59 Å), (Pro8,18)PIIIA (0.76 Å), TIIIA (0.69 Å) and (Pro8,18)TIIIA (0.83 Å). Similar side chain conformations and surface-exposed residues were observed in both the hydroxyproline-containing PIIIA and TIIIA, and their respective proline-containing counterparts, indicating conserved structural features. Both PIIIA and (Pro8,18)PIIIA conotoxin variants populated two distinct conformations in approximately a 3:1 ratio, resulting from *cis-trans* isomerisation at Hyp8/Pro8. In both variants of the TIIIA peptide, Hyp8/Pro8 adopted a *trans* configuration, suggesting that electronic effects of the hydroxyl group do not affect the preference for the *trans* configuration. For the (Pro8,18)TIIIA structure, fewer distance and dihedral angle restraints were obtained compared to the hydroxyproline-containing TIIIA, resulting in higher RMSD values. This suggests that the (Pro8,18)TIIIA structure has lower stability and definition than the native TIIIA structure. This aligns



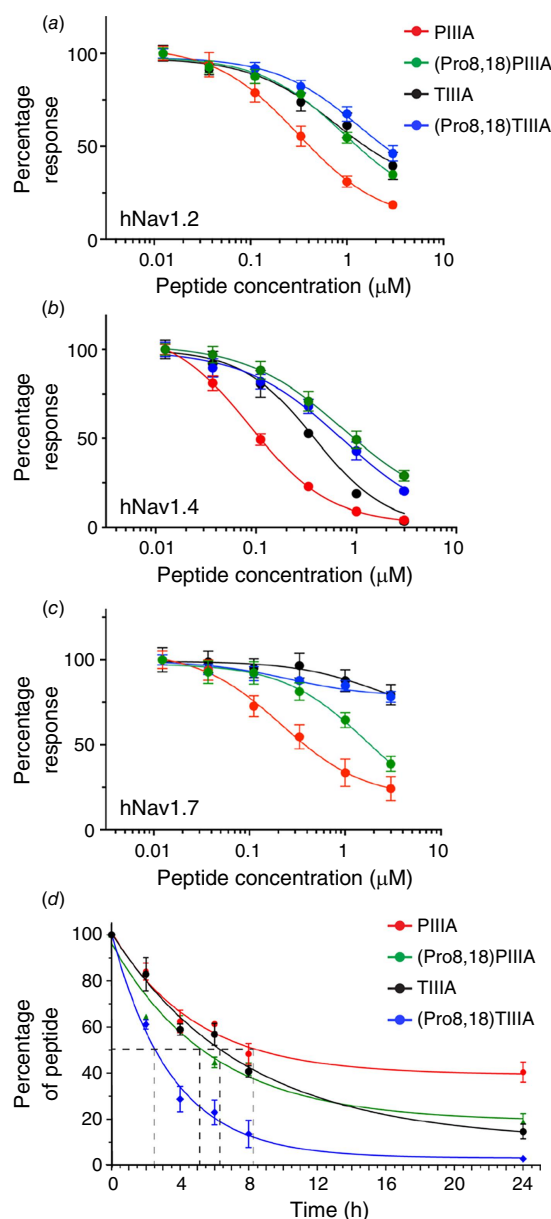
**Fig. 4.** Structural ensembles of PIIIA, (Pro8,18)PIIIA, TIIIA and (Pro8,18)TIIIA. Ensembles of the 20 lowest-energy NMR structures are shown in red (PIIIA), green ((Pro8,18)PIIIA), black (TIIIA) and blue ((Pro8,18)TIIIA), selected based on energy and MolProbity scores. (a) Stick representation of the backbone conformations of the four peptides with cysteine side chains highlighted in yellow to indicate their disulfide connectivities. (b) Cartoon representations of the lowest energy solution NMR structures of the four peptides, highlighting the side chain conformations of the labeled surface-exposed residues.

with the respective folding efficiencies, indicating that although proline is tolerated, it is unfavorable for both folding and structure stabilisation. Perhaps subtle differences between the *cis-trans* isomerisation in Hyp/Pro influence folding by inducing or stabilising helicity in folding intermediates and thereby bringing cysteine pairs into proximity for disulfide bond formation. In all models, the amidated C-terminus bends around towards the peptide backbone. Although we could not compare with the C-terminal acid variants in this study, this has also been observed for C-terminally amidated  $\alpha$ -conotoxins<sup>27</sup> and is probably due to the neutral charge of the amidated C-terminus, which can hydrogen bond with backbone carbonyl groups unlike the negatively charged C-terminal acid.

### Proline hydroxylation increases the electrophysiological activities and stabilities of $\mu$ -conotoxins

To evaluate the impact of proline hydroxylation on the activity of PIIIA and TIIIA, electrophysiological studies were conducted using HEK293 cells expressing various hNav subtypes. The concentration-response curves illustrating the effects of proline hydroxylation in both PIIIA and TIIIA peptides and their proline-containing counterparts are presented in Fig. 5a, with the corresponding  $IC_{50}$  values provided in Supplementary Table S5. The hydroxyproline-containing PIIIA peptide inhibited neuronal voltage-gated sodium channel subtypes hNav1.2, hNav1.7 and muscle subtype hNav1.4 with nanomolar potency (Mean  $IC_{50}$ : 0.33  $\mu$ M at hNav1.2; 0.086  $\mu$ M at hNav1.4; and 0.33  $\mu$ M at hNav1.7), whereas the proline variant (Pro8,18)PIIIA showed a comparatively lower potency across all three hNav subtypes tested (Mean  $IC_{50}$ : 1.02  $\mu$ M at hNav1.2; 0.73  $\mu$ M at hNav1.4; and 1.5  $\mu$ M at hNav1.7). Most prominently, the potency of the hydroxyproline PIIIA variant was  $\sim$ 10-fold higher than (Pro8,18)PIIIA at hNav1.4. The hydroxyproline-containing TIIIA peptide inhibited hNav1.2 and hNav1.4 but had only a limited effect on hNav1.7 (Mean  $IC_{50}$ : 1.55  $\mu$ M at hNav1.2; 0.36  $\mu$ M at hNav1.4; and an incomplete block at 3  $\mu$ M for hNav1.7), indicating a preference for hNav1.2 and 1.4 over hNav1.7. In contrast to the PIIIA variants, the potency of TIIIA was similar to that of the proline variant (Pro8,18)TIIIA (Mean  $IC_{50}$ : 1.57  $\mu$ M at hNav1.2; 0.75  $\mu$ M at hNav1.4; and a partial block at 3  $\mu$ M for hNav1.7). These results suggest that proline hydroxylation in the native PIIIA and TIIIA contributes to activity at hNav1.2 and hNav1.4, with peptide-specific effects.

The stabilities of the four peptide variants in human serum were determined to compare the relative protease stabilities (Fig. 5d). Both hydroxyproline-containing  $\mu$ -conotoxins had higher stability in serum than their corresponding proline variants; after 24 h, more than 40% of the hydroxyproline variant PIIIA remained, whereas only  $\sim$ 27% of the unmodified (Pro8,18)PIIIA variant remained and 25% of the hydroxyproline variant TIIIA remained, compared to less than 10% of the unmodified (Pro8,18)TIIIA. These



**Fig. 5.** Functional activity (potency) and stability of hydroxyproline-containing PIIIA, TIIIA and their proline-containing counterparts (Pro8,18)PIIIA and (Pro8,18)TIIIA. Inhibition of human Nav channels (a) Nav1.2, (b) Nav1.4 and (c) Nav1.7 by hydroxyproline-containing PIIIA and TIIIA peptides in comparison to their proline-containing counterparts (Pro8,18)PIIIA and (Pro8,18)TIIIA, illustrated by the concentration-response relationships for inhibition of  $Na^+$  currents. (d) Serum stabilities of hydroxyproline-containing PIIIA and TIIIA peptides compared to their proline-containing variants, (Pro8,18)PIIIA and (Pro8,18)TIIIA. The percentage of peptide remaining in serum over time is expressed relative to the amount of the respective peptide at the start (0 h). The data are presented as mean  $\pm$  s.e.m. from a minimum of three replicates. Approximate half-lives are shown by dashed lines: PIIIA, 8.3 h; (Pro8,18)PIIIA, 5.2 h; TIIIA, 6.3 h; and (Pro8,18)TIIIA, 2.5 h.

results indicate that proline hydroxylation increases protease stability of both PIIIA and TIIIA  $\mu$ -conotoxins, possibly by subtly stabilising the peptide structures or limiting access to vulnerable protease cleavage sites. In this study, only stability towards serum proteases was investigated; however, stability towards other proteases, e.g. those in gastric fluid, would need to be further investigated for other applications.

## Discussion and conclusion

Solid phase peptide synthesis enabled us to generate all four possible variants of each of the two  $\mu$ -conotoxins PIIA and TIIIA, which would have been difficult to obtain by other methods. Amidation of the C-terminus of these conotoxins appears to be critical for their correct oxidative folding, as we were unable to obtain any correctly folded species of the C-terminal acid variants. We therefore could not directly compare the effects of C-terminal amidation with the corresponding acids but inferred from the structures of the amidated variants that this PTM is essential for neutralising the charge at the terminus and possibly hydrogen bonding with backbone carbonyls.

Proline hydroxylation has a subtle influence on stabilising the structures of both PIIIA and TIIIA; while not drastically altering the overall peptide conformation, proline hydroxylation has pivotal effects in optimising oxidative folding and enhancing proteolytic stability. Multiple conformations were observed for PIIIA, but not for TIIIA, likely because of the  $\alpha$ -helical region between residues 8–12 in PIIIA, in which the Hyp8/Pro8 *cis*–*trans* isomerisation would have a significant effect. The structural effects of hydroxyproline are consistent with earlier findings in other conotoxin families, such as  $\omega$ -conotoxins and  $\alpha$ -conotoxins, in which hydroxylation improved oxidative folding and enhanced structural stability.<sup>18,21</sup>

In this study, proline hydroxylation of both PIIIA and TIIIA influenced the activities at hNavs 1.2, 1.4 and 1.7, possibly by fine-tuning the presentation of pharmacophoric elements critical for channel blockade. This is not the case for all conotoxins; e.g. artificial introduction of hydroxylation in the  $\alpha$ -conotoxins ImI and GI reduced bioactivity.<sup>18</sup> In other studies, arginine 14 has been highlighted as a key residue for high-affinity interactions at the muscle and neuronal subtypes, e.g. for GIIIA and related conotoxins,<sup>28,36,48,49</sup> the functional significance of PTMs is highly context specific. Whereas in conotoxins such as  $\omega$ -conotoxin GVIA<sup>50</sup> and MVIIA,<sup>18</sup> hydroxylation induces pronounced structural rearrangements that directly affect channel binding, in  $\mu$ -conotoxins, the PTMs appear to facilitate subtle improvements in folding and stability that translate into enhanced pharmacological potency. Furthermore, our data on sodium channel inhibition align with earlier studies reporting differential potencies across Nav subtypes,<sup>33</sup> reinforcing the idea that PTMs modulate target selectivity and potency. Taken together, our results showed that hydroxyproline has a more prominent role in the activity and stability of PIIIA compared to TIIIA.

Overall, our findings support the concept that naturally occurring PTMs in  $\mu$ -conotoxins are evolutionarily optimised to enhance folding, stability and biological activity. These insights have broader implications for the development of peptide-based therapeutics. Future studies should further explore the *in vivo* mechanisms governing PTM-dependent folding and activity, including potential chaperone-mediated processes to inform the rational design of ion channel inhibitors. Furthermore, as three-dimensional structures of channel proteins become available through prediction or co-crystal structures, the more precise structure–activity relationships of conotoxin PTMs can be elucidated. By emphasising the necessity of incorporating native PTMs, this work not only explains variability in folding efficiency and bioactivity among conotoxins but also provides a strategic pathway for optimising peptide stability and potency in drug development. Ultimately, these insights pave the way for developing more effective treatments for channelopathies and other related disorders, underscoring the transformative potential of harnessing natural PTMs in therapeutic design.

## Materials and methods

### Solid-phase peptide synthesis

Peptides were synthesised using Fmoc (9-fluorenyl methoxycarbonyl) based solid phase synthesis at a 0.25-mmol scale. The C-terminally amidated peptides, which include the TIIIA, (Pro8,18)TIIIA, PIIIA and (Pro8,18)PIIIA peptides, were synthesised on Rink-Amide 4-Methylbenzhydrylamine hydrochloride (MBHA) resin (0.56 mmol g<sup>-1</sup>) using 0.2 M of Hexafluorophosphate Benzotriazole Tetramethyl Uronium (HBTU) in DMF as coupling reagent. A ratio of 4:4:8 equivalents of amino acid/HBTU/*N,N'*-diisopropylethylamine (DIPEA) was used for each coupling step. Prior to the coupling of each subsequent residue, 20% (v/v) piperidine in DMF was used for the deprotection of the N-terminal amine. Amino acid coupling was done using the automated peptide synthesiser (CS Bio Co. CS336X), with the coupling mixture being applied twice to the resin for all proline, hydroxyproline and cysteine amino acids. After synthesis, a final N-terminal deprotection was carried out using 2- × 5-min reactions of 20% v/v piperidine in DMF and washing with DMF.

The C-terminal acid peptides, which include the TIIIA-OH, (Pro8,18)TIIIA-OH, PIIIA-OH and (Pro8,18)PIIIA-OH peptide chains, were assembled on a 2-chlorotriyl chloride resin at a 0.25-mmol scale. The resin was pre-swelled in DCM for an hour before loading the C-terminal residue. Loading was achieved by applying a solution of 1.2 eq. of Fmoc-protected cysteine and 4 eq. of DIPEA in minimal DCM to the resin. The entire loading process was repeated to achieve adequate loading, with the remaining unreacted resin sites capped using DCM/Methanol (MeOH)/DIPEA (17:2:1), followed by washing with 3 × DCM, 2 × DMF and 2 × DCM at 3-min intervals. Subsequent coupling was done using the automated

peptide synthesiser, with the coupling mixture being applied twice to the resin for all proline, hydroxyproline and cysteine amino acids. After coupling, deprotection using 2- × 5-min reactions of 20% v/v piperidine in DMF was performed before subsequent amino acid coupling.

Upon completion of peptide synthesis, the resin was dried under nitrogen. The peptides were cleaved off the resin and side chain protecting groups released by treatment with a solution of TFA/3,6-dioxo-1,8-octanedithiol/triisopropylsilane/H<sub>2</sub>O (92.5/2.5/2.5/2.5) for 2 h. The cleavage mixture was filtered and rotatory evaporated to remove TFA. Cold diethyl ether was added to the solution and the peptide precipitate was collected by filtration. The peptide pellet was dissolved in a solution of 50/50 Buffer A/B (Buffer A, H<sub>2</sub>O with 0.05% TFA; Buffer B, 90% acetonitrile, 10% H<sub>2</sub>O, 0.045% TFA) before lyophilisation.

Crude peptides were dissolved and filtered, then loaded on a preparative C<sub>18</sub> column (Phenomenex Jupiter 300 Å, 10 µm, 250 × 21.2 mm) and purified using RP-HPLC using an increasing gradient of buffer B in buffer A (1% min<sup>-1</sup> for 80 min) with UV monitoring at 214 and 280 nm. HPLC fractions were collected manually and fractions containing major peaks were analysed by electrospray ionisation mass spectrometry (ESI-MS). Mass/charge ratios of peptide fractions corresponding to the desired peptide molecular weights were collected, and where required, peptides were re-purified until >95% purity. The purity, retention time and peak shapes of peptides in fractions following purification of crude peptides were determined by analytical RP-HPLC on a C18 analytical column (300 Å, 5 m, 2.1-mm inner diameter × 150 mm, Vydac column), at an increasing gradient of buffer B in buffer A (1% min<sup>-1</sup>). Raw mass spectrometry data were analysed using the *Magtran* software (ver. 1.02, see <https://magtran.software.informer.com/>).<sup>51</sup> All peptides were stored in the lyophilised form at -20°C until they were ready for use. Prior to NMR and bioassays, the pure reduced peptides were reconstituted in the appropriate buffers or water. The TIIIA, (Pro8,18)TIIIA, TIIIA-OH, (Pro8,18)TIIIA-OH, peptides were oxidised for 48 h at 0.02 mM in aqueous 0.33 M of NH<sub>4</sub>OAc/0.5 M of GdnHCl at pH 7.8 and 4°C in the presence of both reduced and oxidised glutathione (peptide/GSH/GSSG, 1:100:10 molar ratio), based on conditions previously reported for native TIIIA.<sup>28</sup> The PIIIA, (Pro8,18)PIIIA, PIIIA-OH, (Pro8,18)PIIIA-OH peptides were oxidised at a concentration of 0.02 mM in aqueous 0.33 M of NH<sub>4</sub>OAc, 0.5 M of guanidine HCl. The solution was stirred for 3–5 days at pH 8.1.<sup>29</sup> Purification of oxidised peptides was completed using preparative RP-HPLC chromatography as described for the reduced peptides.

## NMR data collection, processing and structure calculations

Samples of TIIIA, (Pro8,18)TIIIA, TIIIA-OH, (Pro8,18)TIIIA-OH, PIIIA, (Pro8,18)PIIIA, PIIIA-OH and (Pro8,18)PIIIA-OH

peptides were prepared by dissolving ~1 mg of lyophilised, oxidised peptide in 500 µL of solution of H<sub>2</sub>O/D<sub>2</sub>O (90 : 10) at pH ~3.5 before carrying out NMR experiments. The NMR data were acquired on a 700-MHz NMR spectrometer equipped with a helium-cooled cryoprobe. 1-D data of all peptides were recorded and used to assess if a folded form had been achieved. Nuclear Overhauser Spectroscopy (NOESY; mixing time of 200 ms) and 2-D <sup>1</sup>H-<sup>1</sup>H Total Correlation Spectroscopy (TOCSY; mixing time of 80 ms) were obtained at 298 K for folded peptides. A sweep width of 12 ppm, 8 scans and 512 increments were used for TOCSY experiments, and 32 scans and 512 increments were recorded for NOESY experiments. Heteronuclear Single Quantum Coherence (HSQC) experiments (<sup>1</sup>H-<sup>13</sup>C and <sup>1</sup>H-<sup>15</sup>N) were also recorded at natural abundance. By comparing the assigned Ha chemical shifts with the corresponding random coil peptide chemical shifts, the secondary Ha chemical shifts were calculated and the secondary structural features of the peptide were identified.<sup>43</sup> To observe the temperature dependence of the amide protons, further TOCSY data were obtained at different temperatures (288, 293, 298, 303 and 308 K).<sup>46</sup> The data were processed using Bruker Topspin and cross-peak assignment and integration were carried out using CARA ('Computer-Aided Resonance Assignment', see <http://cara.nmr.ch/doku.php/Home>).<sup>52</sup> Resonance assignments were carried out by combining the information from TOCSY and NOESY spectra using sequential assignment strategies.<sup>53</sup> Structural restraints were obtained from the NMR data to attain the three-dimensional structures of the peptides. The interproton distance restraints for the post-translationally modified and unmodified peptides were obtained from the cross-peak volumes in the NOESY spectra. Combined assignment and dynamics algorithm for NMR applications (CYANA) was employed for the automated assignment of NOE cross-peaks, leveraging the identified chemical shifts.<sup>54</sup> TALOS-N was used to predict dihedral  $\phi(C^{-1}-N-C\alpha-C)$  and  $\psi(N-C\alpha-C-N^{+1})$  backbone angles, as well as  $\chi_1(N-C\alpha-C\beta-Xg)$  side chain dihedral angles. Using the program DISH, the TALOS-N backbone dihedral angles were combined with chemical shifts to predict the  $\chi_1(N-C\alpha-C\beta-SX)$  and  $\chi_2(C\alpha-C\beta-SX-SY)$  dihedral angles for the disulfide-bonded cysteine residues.<sup>55</sup> The temperature coefficients of the backbone amide were used to identify hydrogen bond donors. Plotting the chemical shift of the backbone <sup>1</sup>HN proton of each residue *v.* temperature, values greater than -4.6 ppb K<sup>-1</sup> were considered to be suggestive of a hydrogen bond being donated by that specific HN.<sup>45</sup> A set of preliminary structures was calculated from the distance and angle restraint data obtained, using CYANA.<sup>54</sup> The program CNS was then used to calculate structures using the restraints generated by CYANA through automatic assignment, in addition to the dihedral angle restraints from TALOS-N<sup>56</sup> and the hydrogen bond restraints from temperature coefficients and preliminary calculations.<sup>57</sup> Torsion angle dynamics were used by CNS to generate initial structures that were subsequently minimised in explicit water using Cartesian

dynamics. The angle and distance restraints were checked to ensure that there were no violations. The stereochemical quality of the structures was assessed using the *MolProbity* software,<sup>58</sup> which compares geometry to high-quality published structures. A final set of 20 structures from a total calculated 50 were chosen based on *MolProbity* scores, low energy and no violation of dihedral angles or distances greater than 0.2 Å or 3°. *MOLMOL* (ver. 2K.2, see <https://sourceforge.net/projects/molmol/>) was used to display and generate images of the post-translationally modified and unmodified peptides.<sup>60</sup>

## Stability assays

Stability assays for the post-translationally modified TIIIA and its unmodified (Pro8,18)TIIIA variant were carried out in human male pooled serum using a 0.05 mg mL<sup>-1</sup> final peptide concentration. The serum was prepared by centrifugation at 5590g for 10 min at room temperature (25°C) to remove the lipid component and incubated at 37°C for 20 min. Each peptide was incubated at 37°C and aliquots were taken at different time points: 0, 2, 4, 6, 8 and 24 h. Aliquots were quenched by the addition of 15% aqueous trifluoroacetic acid (TFA) and incubated on ice for 30 min. All samples were centrifuged at 14,000g for 10 min at room temperature (25°C) and the supernatant was stored at -20°C until analysis. By contrast, the *in vitro* serum stability of the post-translationally modified PIIIA and its modified (Pro8,18)PIIIA peptide variant was determined by peptide spiking. 30 µL of peptide (1 mg mL<sup>-1</sup>) was added to 570 µL of pooled human male serum to make a final concentration of 0.05 mg mL<sup>-1</sup>. The 100-µL samples were extracted at various intervals and 900 µL of ammonium acetate (0.1 M, pH 3) was added to quench the protease activity. After the samples were placed on ice for 30 min, solid-phase extraction cartridges (Oasis HLB 3cc, Waters) were used to extract the residual peptide. Cartridges were preconditioned with a 70% ACN/1% formic acid (FA) solution (3 mL) before being activated with 6 mL of MeOH for the extraction. Prior to sample loading, the cartridge was equilibrated with 1% FA solution. Following sample loading, 3 mL of 1% FA solution was used for washing and then 3 mL of 30% ACN/1% FA solution was used to elute the peptide variants. Eluted samples were lyophilised and then reconstituted in 200 µL of 1% FA.

Using a linear aqueous acetonitrile 1% gradient containing 0.05% TFA and a flow rate of 0.3 mL min<sup>-1</sup>, the peptide quantification was performed by RP-HPLC on an analytical Grace Vydac C18 column (2.1 mm × 150 mm, 5 mm). The sample absorbance was recorded at 215 nm and the peak area was compared to the peak area at time point 0 h. The remaining peptide amount was expressed as a percentage relative to the recovered peptide amount at time point 0 h. A non-linear fit of one-phase decay in *GraphPad Prism 6* (ver. 6, GraphPad Software, Boston, MA USA) was used to compute the peptide stability.

## Cell culture and automated whole-cell patch-clamp electrophysiology

Human embryonic kidney 293 (HEK293) cells stably expressing recombinant hNav1.2, hNav1.4 and hNav1.7 and the β1 auxiliary subunit (Scottish Biomedical Drug Discovery, Glasgow, UK) were cultured in Minimal Essential medium (MEM) (Sigma–Aldrich, Saint Louis, MO, USA) supplemented with 10% v/v Fetal Bovine Serum (FBS), 2 mM L-glutamine and selected antibiotics as per manufacturer's recommendation. A QPatch 16X automated whole-cell patch clamp device (Sophion Bioscience A/S, Ballerup, Denmark) was used to record Nav channel currents from HEK293 cells that were stably expressing different Nav subtypes and the β1 auxiliary subunit. The cells were cultured for 48 h to reach ~80% confluency, detached using TrypLE Express (trypsin-like protease) and then resuspended to 5 × 10<sup>6</sup> cells mL<sup>-1</sup> in serum-free media (DMEM (Gibco), 25 mM of HEPES, 100 U mL<sup>-1</sup> of penicillin/streptomycin and trypsin inhibitor), following the manufacturer's instructions. The extracellular solution, which was adjusted to pH 7.3 using NaOH, included the following components: 1 mM of CaCl<sub>2</sub>, 1 mM of MgCl<sub>2</sub>, 5 mM of HEPES, 3 mM of KCl, 140 mM of NaCl and 20 mM of TEA-Cl. The intracellular solution contained 140 mM of CsF, 1 mM of EGTA, 5 mM of CsOH, 10 mM of HEPES and 10 mM of NaCl, with CsOH used to adjust the pH to 7.3. Using sucrose, the osmolarity of both solutions was adjusted to 320 mOsm. The compound was prepared in an extracellular solution containing 0.1% bovine serum albumin (Sigma–Aldrich). Cells were kept at a holding potential of -90 mV to acquire the dose-response curves. Na<sup>+</sup> currents were evoked by applying a conditioning pulse of -120 mV for 200 ms, followed by 20-ms voltage steps to 0 mV. Increasing concentrations of the peptide were incubated with the cells at the holding potential for 2 min before the voltage protocol was applied. *GraphPad Prism* (ver. 7.0, GraphPad Software, Boston, MA USA) and *QPatch Assay* software (ver. 5.6.4, Sophion Bioscience, Ballerup, Denmark) were used to analyse the experimental data. For concentration-response curves, a four-parameter Hill equation was employed for fitting, using non-linear regression analysis. Mean IC<sub>50</sub> ± standard error of the mean (s.e.m.) was used to present the results, along with the number of independent experiments provided in triplicate.

## Supplementary material

Supplementary material is available [online](#).

## References

- 1 Norton RS, Olivera BM. Conotoxins down under. *Toxicon* 2006; 48(7): 780–798. doi:10.1016/j.toxicon.2006.07.022
- 2 Lewis RJ, Dutertre S, Vetter I, Christie MJ. Conus venom peptide pharmacology. *Pharmacol Rev* 2012; 64(2): 259–298. doi:10.1124/pr.111.005322
- 3 Jin AH, Muttenthaler M, Dutertre S, Himaya SWA, Kaas Q, Craik DJ, Lewis RJ, Alewood PF. Conotoxins: chemistry and biology. *Chem Rev* 2019; 119(21): 11510–11549. doi:10.1021/acs.chemrev.9b00207

- 4 Kaas Q, Yu R, Jin AH, Dutertre S, Craik DJ. Conoserver: updated content, knowledge, and discovery tools in the conopeptide database. *Nucleic Acids Res* 2012; 40: D325–D330. doi:10.1093/nar/gkr886
- 5 Akondi KB, Muttenthaler M, Dutertre S, Kaas Q, Craik DJ, Lewis RJ, Alewood PF. Discovery, synthesis, and structure-activity relationships of conotoxins. *Chem Rev* 2014; 114(11): 5815–5847. doi:10.1021/cr400401e
- 6 Robinson SD, Norton RS. Conotoxin gene superfamilies. *Mar Drugs* 2014; 12: 6058–6101. doi:10.3390/md12126058
- 7 Norton RS.  $\mu$ -Conotoxins as leads in the development of new analgesics. *Molecules* 2010; 15(4): 2825–2844. doi:10.3390/molecules15042825
- 8 Corpuz GP, Jacobsen RB, Jimenez EC, Watkins M, Walker C, Colledge C, Garrett JE, McDougal O, Li W, Gray WR, *et al.* Definition of the m-conotoxin superfamily: characterization of novel peptides from molluscivorous conus venoms. *Biochemistry* 2005; 44(22): 8176–8186. doi:10.1021/bi047541b
- 9 Knapp O, McArthur JR, Adams DJ. Conotoxins targeting neuronal voltage-gated sodium channel subtypes: potential analgesics? *Toxins* 2012; 4(11): 1236–1260. doi:10.3390/toxins4111236
- 10 Paul George AA, Heimer P, Maaß A, Hamaekers J, Hofmann-Apitius M, Biswas A, Imhof D. Insights into the folding of disulfide-rich  $\mu$ -conotoxins. *ACS Omega* 2018; 3(10): 12330–12340. doi:10.1021/acsomega.8b01465
- 11 McMahon KL, Vetter I, Schroeder CI. Voltage-gated sodium channel inhibition by  $\mu$ -conotoxins. *Toxins* 2024; 16(1): 55. doi:10.3390/toxins16010055
- 12 Dib-Hajj SD, Black JA, Waxman SG. Voltage-gated sodium channels: therapeutic targets for pain. *Pain Med* 2009; 10(7): 1260–1269. doi:10.1111/j.1526-4637.2009.00719.x
- 13 Markgraf R, Leipold E, Schirmeyer J, Paolini-Bertrand M, Hartley O, Heinemann SH. Mechanism and molecular basis for the sodium channel subtype specificity of  $\mu$ -conopeptide CnIIIC. *Br J Pharmacol* 2012; 167(3): 576–586. doi:10.1111/j.1476-5381.2012.02004.x
- 14 Stevens M, Peigneur S, Dyubankova N, Lescrier E, Herdewijn P, Tytgat J. Design of bioactive peptides from naturally occurring  $\mu$ -conotoxin structures. *J Biol Chem* 2012; 287(37): 31382–31392. doi:10.1074/jbc.M112.375733
- 15 Walsh CT, Garneau-Tsodikova S, Gatto GJ Jr. Protein post-translational modifications: the chemistry of proteome diversifications. *Angew Chem Int Ed Engl* 2005; 44(45): 7342–7372. doi:10.1002/anie.200501023
- 16 Conibear AC. Deciphering protein post-translational modifications using chemical biology tools. *Nat Rev Chem* 2020; 4(12): 674–695. doi:10.1038/s41570-020-00223-8
- 17 Buczek O, Bulaj G, Olivera BM. Conotoxins and the post-translational modification of secreted gene products. *Cell Mol Life Sci* 2005; 62(24): 3067–3079. doi:10.1007/s00018-005-5283-0
- 18 Lopez-Vera E, Walewska A, Skalicky JJ, Olivera BM, Bulaj G. Role of hydroxyprolines in the *in vitro* oxidative folding and biological activity of conotoxins. *Biochemistry* 2008; 47(6): 1741–1751. doi:10.1021/bi701934m
- 19 Ekberg J, Craik DJ, Adams DJ. Conotoxin modulation of voltage-gated sodium channels. *Int J Biochem Cell Biol* 2008; 40(11): 2363–2368. doi:10.1016/j.biocel.2007.08.017
- 20 Gorres KL, Raines RT. Prolyl 4-hydroxylase. *Crit Rev Biochem Mol Biol* 2010; 45(2): 106–124. doi:10.3109/10409231003627991
- 21 Bulaj G, Olivera BM. Folding of conotoxins: Formation of the native disulfide bridges during chemical synthesis and biosynthesis of conus peptides. *Antioxid Redox Signal* 2008; 10(1): 141–155. doi:10.1089/ars.2007.1856
- 22 Xu J, Wang Y, Zhang B, Wang B, Du W. Stereochemistry of 4-hydroxyproline affects the conformation of conopeptides. *Chem Commun* 2010; 46(30): 5467–5469. doi:10.1039/c0cc000075b
- 23 Armishaw C, Jensen AA, Balle T, Clark RJ, Harpsøe K, Skonberg C, Liljefors T, Strømgaard K. Rational design of  $\alpha$ -conotoxin analogues targeting  $\alpha_7$  nicotinic acetylcholine receptors: Improved antagonistic activity by incorporation of proline derivatives. *J Biol Chem* 2009; 284(14): 9498–9512. doi:10.1074/jbc.M806136200
- 24 Prigge ST, Mains RE, Eipper BA, Amzel LM. New insights into copper monooxygenases and peptide amidation: Structure, mechanism and function. *Cell Mol Life Sci* 2000; 57(8–9): 1236–1259. doi:10.1007/pl00000763
- 25 Wen J, Adams DJ, Hung A. Interactions of the  $\alpha_3\beta_2$  nicotinic acetylcholine receptor interfaces with  $\alpha$ -conotoxin Isia and its carboxylated c-terminus analogue: molecular dynamics simulations. *Mar Drugs* 2020; 18(7): 349. doi:10.3390/md18070349
- 26 Liu X, Yao G, Wang K, Liu Y, Wan X, Jiang H. Structural and functional characterization of conotoxins from conus achatinus targeting NMDAR. *Mar Drugs* 2020; 18(3): 135. doi:10.3390/md18030135
- 27 Ho TNT, Lee HS, Swaminathan S, Goodwin L, Rai N, Ushay B, Lewis RJ, Rosengren KJ, Conibear AC. Posttranslational modifications of  $\alpha$ -conotoxins: sulfotyrosine and C-terminal amidation stabilise structures and increase acetylcholine receptor binding. *RSC Med Chem* 2021; 12(9): 1574–1584. doi:10.1039/d1md00182e
- 28 Lewis RJ, Schroeder CI, Ekberg J, Nielsen KJ, Loughnan M, Thomas L, Adams DA, Drinkwater R, Adams DJ, Alewood PF. Isolation and structure-activity of  $\mu$ -conotoxin TIIIA, a potent inhibitor of tetrodotoxin-sensitive voltage-gated sodium channels. *Mol Pharmacol* 2007; 71(3): 676–685. doi:10.1124/mol.106.028225
- 29 Nielsen KJ, Watson M, Adams DJ, Hammarström AK, Gage PW, Hill JM, Craik DJ, Thomas L, Adams D, Alewood PF, *et al.* Solution structure of  $\mu$ -conotoxin PIIIA, a preferential inhibitor of persistent tetrodotoxin-sensitive sodium channels. *J Biol Chem* 2002; 277(30): 27247–27255. doi:10.1074/jbc.M201611200
- 30 Clark RJ, Fischer H, Dempster L, Daly NL, Rosengren KJ, Nevin ST, Meunier FA, Adams DJ, Craik DJ. Engineering stable peptide toxins by means of backbone cyclization: stabilization of the  $\alpha$ -conotoxin MII. *Proc Natl Acad Sci USA* 2005; 102(39): 13767–13772. doi:10.1073/pnas.0504613102
- 31 Armishaw CJ, Singh N, Medina-Franco JL, Clark RJ, Scott KC, Houghten RA, Jensen AA. A synthetic combinatorial strategy for developing  $\alpha$ -conotoxin analogs as potent  $\alpha_7$  nicotinic acetylcholine receptor antagonists. *J Biol Chem* 2010; 285(3): 1809–1821. doi:10.1074/jbc.M109.071183
- 32 Chan LY, Gunasekera S, Henriques ST, Worth NF, Le SJ, Clark RJ, Campbell JH, Craik DJ, Daly NL. Engineering pro-angiogenic peptides using stable, disulfide-rich cyclic scaffolds. *Blood* 2011; 118(25): 6709–6717. doi:10.1182/blood-2011-06-359141
- 33 Wilson MJ, Yoshikami D, Azam L, Gajewiak J, Olivera BM, Bulaj G, Zhang MM.  $\mu$ -Conotoxins that differentially block sodium channels nav1.1 through 1.8 identify those responsible for action potentials in sciatic nerve. *Proc Natl Acad Sci USA* 2011; 108(25): 10302–10307. doi:10.1073/pnas.1107027108
- 34 Khoo KK, Gupta K, Green BR, Zhang MM, Watkins M, Olivera BM, Balam P, Yoshikami D, Bulaj G, Norton RS. Distinct disulfide isomers of  $\mu$ -conotoxins KIIIA and KIIIB block voltage-gated sodium channels. *Biochemistry* 2012; 51(49): 9826–9835. doi:10.1021/bi301256s
- 35 Smallwood TB, Krumpke LRH, Payne CD, Klein VG, O’Keefe BR, Clark RJ, Schroeder CI, Rosengren KJ. Picking the tyrosine-lock: chemical synthesis of the tyrosyl-DNA phosphodiesterase i inhibitor recifin a and analogues. *Chem Sci* 2024; 15(33): 13227–13233. doi:10.1039/d4sc01976h
- 36 Shon KJ, Olivera BM, Watkins M, Jacobsen RB, Gray WR, Floresca CZ, Cruz LJ, Hillyard DR, Brink A, Terlau H, *et al.*  $\mu$ -Conotoxin PIIIA, a new peptide for discriminating among tetrodotoxin-sensitive Na channel subtypes. *J Neurosci* 1998; 18(12): 4473–4481. doi:10.1523/jneurosci.18-12-04473.1998
- 37 Bax A, Davis DG. Mlev-17-based two-dimensional homonuclear magnetization transfer spectroscopy. *J Magn Reson* 1985; 65(2): 355–360. doi:10.1016/0022-2364(85)90018-6
- 38 Kumar A, Ernst RR, Wüthrich K. A two-dimensional nuclear overhauser enhancement (2D NOE) experiment for the elucidation of complete proton-proton cross-relaxation networks in biological macromolecules. *Biochem Biophys Res Commun* 1980; 95(1): 1–6. doi:10.1016/0006-291x(80)90695-6
- 39 Jeener J, Meier BH, Bachmann P, Ernst RR. Investigation of exchange processes by two-dimensional NMR spectroscopy. *J Chem Phys* 1979; 71(11): 4546–4553. doi:10.1063/1.438208
- 40 Vuister GW, Bax A. Resolution enhancement and spectral editing of uniformly  $^{13}\text{C}$ -enriched proteins by homonuclear broadband  $^{13}\text{C}$  decoupling. *J Magn Reson* 1992; 98(2): 428–435. doi:10.1016/0022-2364(92)90144-v
- 41 Palmer AG, Cavanagh J, Wright PE, Rance M. Sensitivity improvement in proton-detected two-dimensional heteronuclear correlation

- NMR spectroscopy. *J Magn Reson* 1991; 93(1): 151–170. doi:10.1016/0022-2364(91)90036-s
- 42 Wüthrich K. *NMR of proteins and nucleic acids*. Wiley; 1986.
- 43 Wishart DS, Bigam CG, Holm A, Hodges RS, Sykes BD.  $^1\text{H}$ ,  $^{13}\text{C}$  and  $^{15}\text{N}$  random coil NMR chemical shifts of the common amino acids. I. Investigations of nearest-neighbor effects. *J Biomol NMR* 1995; 5(1): 67–81. doi:10.1007/BF00227471
- 44 Conibear AC, Rosengren KJ, Becker CFW, Kaehlig H. Random coil shifts of posttranslationally modified amino acids. *J Biomol NMR* 2019; 73(10–11): 587–599. doi:10.1007/s10858-019-00270-4
- 45 Cierpicki T, Otlewski J. Amide proton temperature coefficients as hydrogen bond indicators in proteins. *J Biomol NMR* 2001; 21(3): 249–261. doi:10.1023/a:1012911329730
- 46 Schroeder CI, Rosengren KJ. Three-dimensional structure determination of peptides using solution nuclear magnetic resonance spectroscopy. *Methods Mol Biol* 2020; 2068: 129–162. doi:10.1007/978-1-4939-9845-6\_7
- 47 Williams CJ, Headd JJ, Moriarty NW, Prisant MG, Videau LL, Deis LN, Verma V, Keedy DA, Hintze BJ, Chen VB, Jain S, Lewis SM, Arendall WB III, Snoeyink J, Adams PD, Lovell SC, Richardson JS, Richardson DC. *MolProbity*: more and better reference data for improved all-atom structure validation. *Protein Sci* 2018; 27(1): 293–315. doi:10.1002/pro.3330
- 48 Dudley SC Jr, Todt H, Lipkind G, Fozzard HA. A  $\mu$ -conotoxin-insensitive  $\text{Na}^+$  channel mutant: possible localization of a binding site at the outer vestibule. *Biophys J* 1995; 69(5): 1657–1665. doi:10.1016/s0006-3495(95)80045-7
- 49 Chang NS, French RJ, Lipkind GM, Fozzard HA, Dudley S Jr. Predominant interactions between  $\mu$ -conotoxin arg-13 and the skeletal muscle  $\text{Na}^+$  channel localized by mutant cycle analysis. *Biochemistry* 1998; 37(13): 4407–4419. doi:10.1021/bi9724927
- 50 Pallaghy PK, Norton RS. Refined solution structure of  $\omega$ -conotoxin GVIA: implications for calcium channel binding. *J Pept Res* 1999; 53(3): 343–351. doi:10.1034/j.1399-3011.1999.00040.x
- 51 Zhang Z, Marshall AG. A universal algorithm for fast and automated charge state deconvolution of electrospray mass-to-charge ratio spectra. *J Am Soc Mass Spectrom* 1998; 9(3): 225–233. doi:10.1016/s1044-0305(97)00284-5
- 52 Keller R. *The computer aided resonance assignment tutorial*. Goldau, Switzerland: CANTINA Verlag; 2004.
- 53 Wüthrich K, Wider G, Wagner G, Braun W. Sequential resonance assignments as a basis for determination of spatial protein structures by high resolution proton nuclear magnetic resonance. *J Mol Biol* 1982; 155(3): 311–319. doi:10.1016/0022-2836(82)90007-9
- 54 Güntert P. Automated NMR structure calculation with CYANA. *Methods Mol Biol* 2004; 278: 353–378. doi:10.1385/1-59259-809-9:353
- 55 Armstrong DA, Kaas Q, Rosengren KJ. Prediction of disulfide dihedral angles using chemical shifts. *Chem Sci* 2018; 9(31): 6548–6556. doi:10.1039/C8SC01423J
- 56 Shen Y, Bax A. Protein backbone and sidechain torsion angles predicted from NMR chemical shifts using artificial neural networks. *J Biomol NMR* 2013; 56(3): 227–241. doi:10.1007/s10858-013-9741-y
- 57 Brünger AT, Adams PD, Clore GM, DeLano WL, Gros P, Grosse-Kunstleve RW, Jiang JS, Kuszewski J, Nilges M, Pannu NS, et al. Crystallography & NMR system: a new software suite for macromolecular structure determination. *Acta Crystallogr – D. Biol Crystallogr* 1998; 54(Pt 5): 905–921. doi:10.1107/s0907444998003254
- 58 Davis IW, Leaver-Fay A, Chen VB, Block JN, Kapral GJ, Wang X, Murray LW, Arendall WB, Snoeyink J, Richardson JS, Richardson DC. *MolProbity*: all-atom contacts and structure validation for proteins and nucleic acids. *Nucleic Acids Res* 2007; 35: W375–W383. doi:10.1093/nar/gkm216
- 59 Chen VB, Arendall WB III, Headd JJ, Keedy DA, Immormino RM, Kapral GJ, Murray LW, Richardson JS, Richardson DC. *MolProbity*: all-atom structure validation for macromolecular crystallography. *Acta Crystallogr – D. Biol Crystallogr* 2010; 66(Pt 1): 12–21. doi:10.1107/s0907444909042073
- 60 Koradi R, Billeter M, Wüthrich K. *MOLMOL*: a program for display and analysis of macromolecular structures. *J Mol Graph* 1996; 14(1): 51–55. doi:10.1016/0263-7855(96)00009-4

**Data availability.** The data used to generate the results in this manuscript are available upon request from the authors.

**Conflicts of interest.** The authors declare that they have no conflicts of interest.

**Declaration of funding.** This work was supported by the Australian Government Research Training Program (RTP) scholarship awarded to Victoria Adegeke. This research was funded in part by the Austrian Science Fund (FWF) (grant DOI:10.55776/P36101) to Anne Conibear.

**Acknowledgements.** The authors thank the School of Biomedical Science, the Centre for Advanced Imaging, and the Institute of Molecular Biosciences at The University of Queensland for providing facilities and technical support services. Open Access publication was supported by The University of Queensland library through an agreement between The University of Queensland and CSIRO Publishing. The authors also thank Tobias Gökler (TU Wien) for helpful feedback and discussions.

#### Author affiliations

<sup>A</sup>School of Biomedical Sciences, Faculty of Medicine, The University of Queensland, Saint Lucia, Qld 4072, Australia.

<sup>B</sup>Institute for Molecular Bioscience, The University of Queensland, Saint Lucia, Qld 4072, Australia.

<sup>C</sup>Institute of Applied Synthetic Chemistry, Faculty of Technical Chemistry, TU Wien, Getreidemarkt 9, A-1060 Vienna, Austria.